Nanotechnology **19** (2008) 455605 (5pp) doi:10.1088/0957-4484/19/45/455605

# Effective growth of boron nitride nanotubes by thermal chemical vapor deposition

**Chee Huei Lee[1], Jiesheng Wang[1], Vijaya K Kayatsha[1], Jian Y Huang[2] and Yoke Khin Yap[1,3]**

[1] Department of Physics, Michigan Technological University, 1400 Townsend Drive, Houghton, MI 49931, USA
[2] Center for Integrated Nanotechnologies (CINT), Sandia National Laboratories, Albuquerque, NM 87185, USA

E-mail: ykyap@mtu.edu

Received 15 August 2008, in final form 16 September 2008
Published 9 October 2008
Online at stacks.iop.org/Nano/19/455605

**Abstract**
Effective growth of multiwalled boron nitride nanotubes (BNNTs) has been obtained by thermal chemical vapor deposition (CVD). This is achieved by a growth vapor trapping approach as guided by the theory of nucleation. Our results enable the growth of BNNTs in a conventional horizontal tube furnace within an hour at 1200 °C. We found that these BNNTs have an absorption band edge of 5.9 eV, approaching that of single h-BN crystals, which are promising for future nanoscale deep-UV light emitting devices.

(Some figures in this article are in colour only in the electronic version)

Boron nitride nanotubes (BNNTs) were theoretical prediction in 1994 [1, 2] and experimental realization in the following year [3]. Like carbon nanotubes (CNTs), BNNTs posess extraordinary structural and mechanical properties. In addition, BNNTs have a higher oxidation resistance than CNTs and a wider bandgap (∼5.5 eV) that is insensitive to tube diameter, number of walls and chirality [2]. In the past decade, BNNTs have been grown by arc discharge [3–5], laser ablation [6], substitution reaction of BN atoms from CNT template [7], ball-milling [8], and chemical vapor deposition (CVD) using borazine [9]. However, these techniques either require high growth temperatures or dangerous chemicals, and the products are filled with impurities. Recently, we have successfully carried out the low temperature growth of pure BNNTs at 600 °C by a plasma-enhanced pulsed-laser deposition (PE-PLD) technique [10]. For the first time, our PE-PLD technique enabled the direct growth of vertically-aligned BNNTs on substrates with controllable patterns. However, all these reported techniques required specific experimental systems that are not commonly used for the growth of other nanostructures like CNTs and nanowires. This situation has limited the experimental study of the properties of BNNTs.

[3] Author to whom any correspondence should be addressed.

Apparently, convenient growth techniques for BNNTs are desired in order to enhance future investigation on the properties and the applications of BNNTs. The most prospective approach is thermal CVD, which has gained popularity for the growth of CNTs and various ZnO nanostructures. The boric oxide CVD (BOCVD) method is considered as a significant advancement for the synthesis of BNNTs [11, 12]. In the BOCVD technique, B, MgO and other metal oxides are used as the precursors. Induction heating is applied to activate the precursors at temperature >1300 °C. Volatile $B_xO_y$ vapors generated in these reactions is carried by Ar gas to interact with ammonia gas to form BNNTs. This technique requires a specially designed vertical induction furnace with rapid heating and a large temperature gradient.

Here we demonstrate a simple approach for the growth of BNNTs in a conventional horizontal tube furnace consisting of a quartz tube vacuum chamber. A similar growth system has been commonly used for the synthesis of CNTs [13, 14] and various ZnO nanostructures [15, 16]. Thus we think that our approach can be easily reproduced by researchers working on the growth of CNTs and nanowires and enhance the research activity of BNNTs. The essential accessory of our experimental setup is a quartz test tube which is 60 cm

 

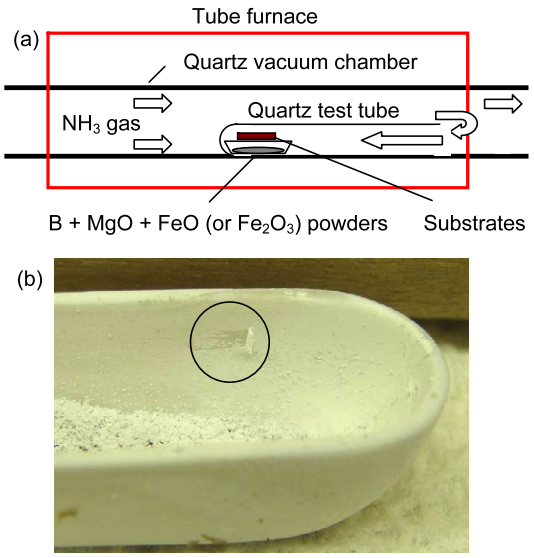


**Figure 1.** (a) Experimental setup for the growth of BNNTs in a horizontal tube furnace. (b) A photograph of the precursor materials in the alumina boat coated with a white layer of BNNTs. These BNNTs can be easily collected by mechanical scratching (marked by a circle).

long and 2 cm in diameter (figure 1(a)). A mixture of B, MgO and FeO (or $Fe_2O_3$) powders were used as the precursor materials and were placed near the closed-end of the test tube. The molar ratio of B:MgO:FeO (or $Fe_2O_3$) is fixed at 2:1:1 for all experiments. A total of 100 mg of these powders were placed in an alumina combustion boat and loaded into the quartz vacuum chamber so that the closed-end of the test tube is located at the center of the heating zone as shown in figure 1(a). Several substrates can be placed on top of the alumina boat for the deposition of BNNTs. The quartz tube chamber was evacuated to about ∼30 mTorr before 200 sccm of $NH_3$ gas was flowed into the chamber. Subsequently, the precursors were heated to 1200 °C and held for 1 h. At this temperature, reactive $B_xO_y$ vapors will be generated and react with $NH_3$ gas to form BNNTs. We believed that FeO (or $Fe_2O_3$) and MgO are serving as the catalyst for these reactions. White coatings (BNNTs) can be observed on the precursor materials, on the test tube, and around the inner side walls of the alumina boat (figure 1(b)). These BNNTs can also be coated on substrates placed on top of the combustion boat.

Figure 2(a) is a scanning electron microscopy (SEM) (Hitachi S-4700) image, which shows the morphologies of the as-grown BNNTs. Clean and long BNNTs can be clearly observed on the as-grown products. The typical diameter of these tubes is range from 10 to 100 nm, depending on the experiment parameters. The length is estimated to be longer than 10 $\mu$m. Transmission electron microscopy (TEM) indicates that these BNNTs contain high-order tubular structures (figures 2(b) and (c)), with some amorphous BN coatings on the side walls. Energy filtered imaging was applied to identify the compositional property of these BNNTs. As shown in figure 2(d), the mapping of boron and nitrogen atoms indicate that this is a BNNT. Carbon is not detected since no carbon source was used in the growth. This was then reconfirmed by electron energy loss spectroscopy (EELS). As shown in figure 2(e), sharp boron and nitrogen K-edge bands

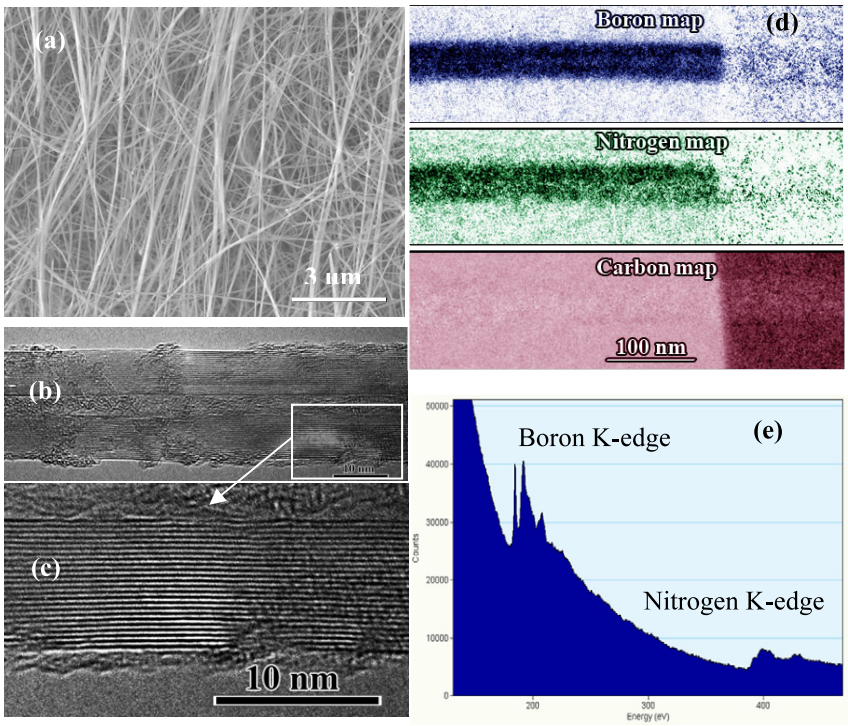


**Figure 2.** (a) SEM images of the as-grown BNNTs and their typical TEM images at (b) low and (c) high magnification. (d) Energy filtered imaging shown that these nanotubes consist of boron and nitrogen atoms but not carbon. This is confirmed by (e) electron energy loss spectroscopy (EELS).

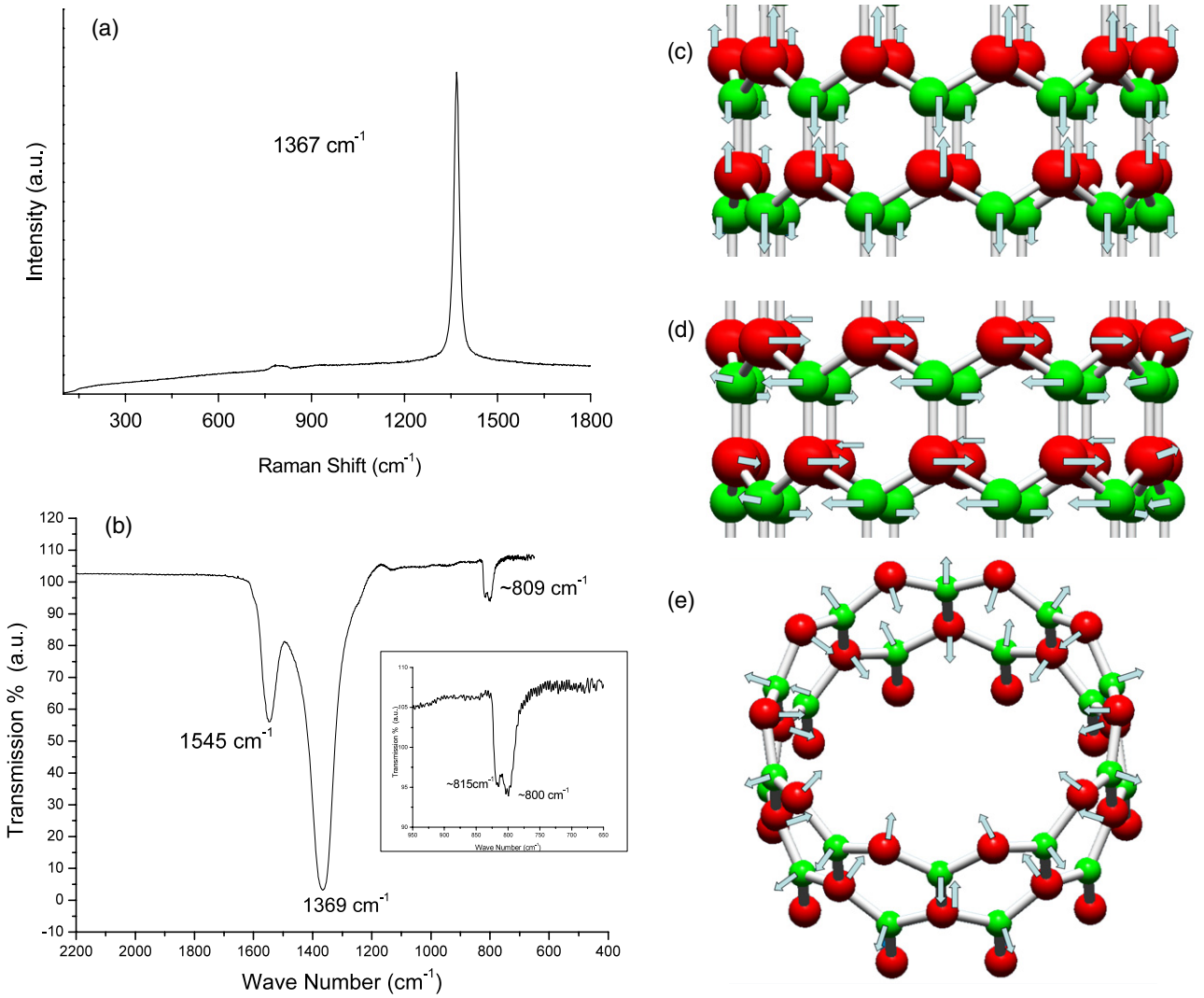


**Figure 3.** (a) Raman and (b) FTIR spectra of BNNTs. (c) Vibration mode along the longitudinal (L) or tube axis of a BNNT which corresponds to ∼1369 $cm^{-1}$. (d) Vibration mode along the tangential (T) directions of a BNNT at ∼1545 $cm^{-1}$. (e) The out-of-plane radial buckling (R) mode of a BNNT at ∼809 $cm^{-1}$.

were detected, which composed of both the $\pi^*$ and $\sigma^*$ peaks that are typical for $sp^2$ bonded BN networks.

The as-grown BNNT samples were also characterized by Raman and Fourier transformed infrared (FTIR) spectroscopy. Raman spectra were collected as excited by a HeCd ($\lambda$ = 325 nm) laser (Jobin-Yvon LabRAM HR800). A sharp Raman peak at ∼1367 $cm^{-1}$ can be detected (figure 3(a)), which corresponds to the well-known $E_{2g}$ in-plane vibrational mode of the hexagonal BN (h-BN) networks. The FTIR spectra were taken in a transmission mode on BNNTs dispersed on a thin Si substrate under a FTIR microscope (Jasco IRT-3000). We correlate our FTIR spectrum of BNNTs with the reported *ab initio* calculations that demonstrate the IR active modes by the zone-folding method [17, 18]. Although these theoretical works are based on isolated single wall tubes, it has been justified that the effect of bundling on the phonon frequency is low [17, 18]. Experimentally, we found that the effect of multiwalled nanotubes on the phonon frequency is insignificant. As shown in figure 3(b), three absorption frequency regimes can be obviously distinguishable at ∼809, ∼1369, and ∼1545 $cm^{-1}$.

The absorption bands at ∼1369 and ∼1545 $cm^{-1}$ are attributed to the in-plane stretching modes of the hexagonal BN (h-BN) networks. This has been explained by the zone-folding method, which considered BNNTs as the seamless cylindrical rolls of h-BN sheets [17]. The intense ∼1369 $cm^{-1}$ band is corresponding to the transverse optical (TO) mode of h-BN sheets that vibrates along the longitudinal (L) or tube axis of a BNNT, as shown in figure 3(c). The absorption band at ∼1545 $cm^{-1}$ is assigned to the stretching of the h-BN network along the tangential (T) directions of a BNNT (see figure 3(d)). This stretching mode is corresponding to the longitudinal optical (LO) mode of the h-BN sheets, which is Raman inactive. It is also worth noting that this LO mode smears out for h-BN bulks or thin films, and only shows up when the tube curvature induces a strain on the h-BN networks. Thus, we suggest that only highly crystalline BNNTs would show up this LO mode. In addition, we note that the T mode

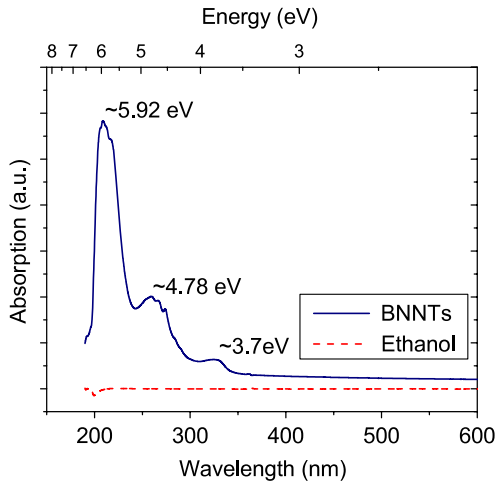


**Figure 4.** UV–visible absorption spectra of the as-grown BNNTs suspended in ethanol.

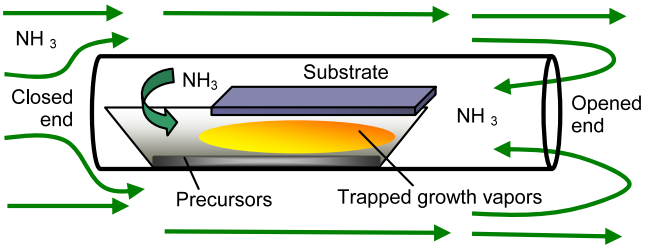


**Figure 5.** Reactive growth vapor trapping by the test tube and the partially covered combustion boat.

vibration may shift between ~1530 and ~1545 $cm^{-1}$, from sample to sample. This is explained by the change of the average diameter of BNNTs in different samples, attributed to different curvatures of the h-BN sheets in BNNTs and thus the induced lattice strains along the tangential directions of the nanotubes as can be visualized in figure 3(d).

The weak absorption at ~809 $cm^{-1}$ is associated with the out-of-plane radial buckling (R) mode where boron and nitrogen atoms are moving radially inward or outward (as illustrated in figure 3(e)) [17]. This interpretation is also identical to the out-of-plane bending mode of h-BN films [19] with a small shift in wavenumber due to the strain developed on the tubular h-BN network in BNNTs. More interestingly, we always observe a splitting of this R mode vibration at ~800 and ~815 $cm^{-1}$, as highlighted in the inset of figure 3(b). Tentatively, we think that the splitting of the radial buckling vibration is related to the complex interaction of buckling vibration at different h-BN sheets that have different diameters and chiralities. However, the origin of this splitting will require further theoretical and experimental analysis in the future.

UV–visible absorption spectroscopy (HP 8453 Spectrophotometer) was also used to further characterize the as-grown BNNTs. This was performed by a suspension of BNNTs in ethanol. As shown in figure 4, a strong absorption at ~5.9 eV was detected. This is corresponding to the optical bandgap of BNNTs. The absorption band at ~4.75 eV is due to the intrinsic dark exciton absorption, which is in very good agreement with the theoretical calculation [20, 21]. We suggest that the relatively small absorption at ~3.7 eV may be associated with defects of the BNNTs [22]. The optical band gap detected here is larger than that reported for BNNTs (5.5 eV) grown by BOCVD in induction furnaces at higher growth temperatures [22]. The bandgap of our BNNTs is comparable to that of single wall BNNTs [23] and hexagonal BN single crystals [24].

The success of our experiments in fact is guided by the theory of nucleation [15, 25]. The probability of nuclei formation is given by $P_N = A\exp(\frac{-\pi\sigma^2}{k^2T^2\ln\alpha})$, where $A$ is a constant, $\sigma$ is the surface energy, $\alpha - 1$ is the supersaturation, where $\alpha = p/p_o$. In this case $p$ is the vapor pressure of the growth species, $p_o$ is the equilibrium vapor pressure of the condensed phase, $k$ is the Boltzmann constant, and $T$ is the temperature in Kelvin. In other words, at constant growth conditions, $T$ and assuming a constant surface energy ($\sigma$) throughout the experiment, it is possible to enhance $\alpha$ and the nucleation probability ($P_N$) of both the catalyst particles and BNNTs by trapping the reactive vapor pressure ($p$) to a critical level. In our case, the surface energy is referring to that of the catalyst particles which induce the formation of BNNTs. Higher vapor pressures (and thus $\alpha$) are proven to enhance the yield of BNNTs in a series of experiments with more precursor powders. The details will be discussed in the future. It is notable that the yield of BNNTs is also higher when the combustion boat is partially covered by substrates, as illustrated in figure 5. As shown, the small closed-end quartz tube and the substrates on top of the combustion boat help to accumulate and trap the growth vapors so as to increase the nucleation rates of BNNTs which react with $NH_3$ gas. Besides, the close-end quartz tube is placed in such a way that the open end is faced against the $NH_3$ flow. This configuration avoids direct $NH_3$ flow across the reaction zone and prevents the reactive growth vapors being carried away before reaching the critical vapor pressure for effective nucleation of BNNTs. $NH_3$ gas can diffuse into the reaction zone from the opened-end of the test tube for the nucleation and growth of BNNTs. We have experimentally verified that BNNTs can not be grown when the closed-end quartz was replaced with an opened-end tube.

Although the success of our experiments is based on the enhanced nucleation rate of the catalyst, the nucleation theory does not provide information about the growth mechanism of the BNNTs. We propose that the growth of BNNTs is based on the vapor–liquid–solid (VLS) mechanism [26]. During the reaction of the precursor powders, growth vapors containing both BN and catalyst species are generated. When the vapor pressure is sufficient, the catalyst vapors will condense into liquid (or partially melted) particles.The BN species will start to dissolve into the catalyst, cause supersaturation and lead to the precipitation of BNNTs. The formation of these BNNTs depends on the sizes of these catalyst particles and the partial pressure of BN growth species. Apparently within the tested range of our experimental parameters, these particles are within the appropriate nanoscale that enables the formation of BNNTs described here. Larger droplets could also be

condensed but these particles did not lead to the growth of large diameter BNNTs since they require more BN growth species to cause supersaturation.

In summary, we have demonstrated a simple procedure for effective growth of BNNTs in a conventional horizontal tube furnace. This was obtained by trapping the reactive growth vapors using a closed-end test tube, as guided by the theory of nucleation. Our procedures can be easily reproduced by others and thus will promote future research activity on BNNTs.

## Acknowledgments

This project is supported by National Science Foundation *CAREER* award (award number 0447555). VKK is supported by the US Department of Energy, the Office of Basic Energy Sciences (Grant No. DE-FG02-06ER46294). This work was performed, in part, at the Center for Integrated Nanotechnologies, a US Department of Energy, Office of Basic Energy Sciences user facility. Sandia National Laboratories is a multi-program laboratory operated by Sandia Corporation, a Lockheed-Martin Company, for the US Department of Energy under Contract No DE-AC04-94AL85000.

## References

[1] Rubio A, Corkill J L and Cohen M L 1994 *Phys. Rev.* B **49** 5081
[2] Blase X, Rubio A, Louie S G and Cohen M L 1994 *Europhys. Lett.* **28** 335
[3] Chopra N G, Luyken R J, Cherrey K, Crespi V H, Cohen M L, Louie S G and Zettl A 1995 *Science* **269** 966
[4] Terrones M *et al* 1996 *Chem. Phys. Lett.* **259** 568
[5] Loiseau A, Willaime F, Demoncy N, Hug G and Pascard H 1996 *Phys. Rev. Lett.* **76** 4737
[6] Yu D P, Sun X S, Lee C S, Bello I, Lee S T, Gu H D, Leung K M, Zhou G W, Dong Z F and Zhang Z 1998 *Appl. Phys. Lett.* **72** 1966
[7] Han W, Bando Y, Kurashima K and Sato T 1998 *Appl. Phys. Lett.* **73** 3085
[8] Chen Y, Chadderton L T, Gerald J F and Williams J S 1999 *Appl. Phys. Lett.* **74** 2960
[9] Lourie O R, Jones C R, Bartlett B M, Gibbons P C, Ruoff R S and Buhro W E 2000 *Chem. Mater.* **12** 1808
[10] Wang J, Kayastha V K, Yap Y K, Fan Z, Lu J G, Pan Z, Ivanov I N, Puretzky A A and Geohegan D B 2005 *Nano Lett.* **5** 2528
[11] Tang C, Bando Y, Sato T and Kurashima K 2002 *Chem. Commun.* 1290
[12] Zhi C, Bando Y, Tan C and Golberg D 2005 *Solid State Commun.* **135** 67
[13] Kayastha V K, Wu S, Moscatello J and Yap Y K 2007 *J. Phys. Chem.* C **111** 10158
[14] Kayastha V, Yap Y K, Dimovski S and Gogotsi Y 2004 *Appl. Phys. Lett.* **85** 3265
[15] Mensah S L, Kayastha V K, Ivanov I N, Geohegan D B and Yap Y K 2007 *Appl. Phys. Lett.* **90** 113108
[16] Mensah S L, Kayastha V K and Yap Y K 2007 *J. Phys. Chem.* C **111** 16092
[17] Wirtz L, Rubio A, de la Concha R A and Loiseau A 2003 *Phys. Rev.* B **68** 045425
[18] Wirtz L and Rubio A 2003 *IEEE Trans. Nanotechnol.* **2** 341
[19] Wang J and Yap Y K 2006 *Diamond Relat. Mater.* **15** 444
[20] Park C-H, Spataru C D and Louie S G 2006 *Phys. Rev. Lett.* **96** 126105
[21] Wirtz L, Marini A and Rubio A 2006 *Phys. Rev. Lett.* **96** 126104
[22] Jaffrennou P, Barjon J, Lauret J S, Maguer A, Golberg D, Attal-Trétout B, Ducastelle F and Loiseau A 2007 *Phys. Status Solidi* b **244** 4147
[23] Arenal R, Stephan O, Kociak M, Taverna D, Loiseau A and Colliex C 2005 *Phys. Rev. Lett.* **95** 127601
[24] Kubota Y, Watanabe K, Tsuda O and Taniguchi T 2007 *Science* **317** 932
[25] Blakely J M and Jackson K A 1962 *J. Chem. Phys.* **37** 428
[26] Wagner G W and Ellis W C 1964 *Appl. Phys. Lett.* **4** 89